On the capture width of wave energy converters

A.A.E. Price[a,*], C.J. Dent[a], A.R. Wallace[a]

[a] *Institute for Energy Systems, The University of Edinburgh, Edinburgh, EH9 3JL, United Kingdom*

Abstract

This paper extends the theory on capture width, a commonly used performance indicator for a wave energy converter (WEC). The capture width of a linear WEC is shown to depend on two properties: the spectral power fraction (a property introduced in this paper), which depends entirely on the sea-state, and the monochromatic capture width, which is determined by the geometry of the WEC and the chosen power take off (PTO) coefficients. Each of these properties is examined in detail. Capture width is shown to be a measure of how well these two properties coincide. Their interaction confirms accepted practices in the design of WECs. A study of the effects of PTO control on the capture width suggests that geometry control, a form of control that has not been the focus of much academic research, despite its use in the wave energy industry, deserves more attention. The distinction between PTO control and geometry control is outlined. While capture width is a valuable design tool, its limitations must be recognised. The assumptions made in the formulation of capture width are listed, and its limitations as a tool for estimating annual power capture of a WEC are discussed.

Key words: control, wave energy, capture width
PACS: 45.20.Dg, 45.30.+s, 45.80.+r

1. Introduction

Capture width is a parameter that characterises the performance of a wave energy converter (WEC). It is the width of the wave-front (assuming uni-directional waves) that contains the same amount of power as that absorbed by the WEC. As the capture width depends very much on the size (scale) of the WEC, a commonly used related quantity is the relative capture width. This is the capture width normalised by the characteristic width of the WEC; the width of the device encountered by the oncoming waves, that is, along the line orthogonal to (uni-directional) wave propagation. The relative capture width

*Corresponding author
Email addresses: Ally.Price@ed.ac.uk (A.A.E. Price), Chris.Dent@ed.ac.uk (C.J. Dent), robin.wallace@ed.ac.uk (A.R. Wallace)

Physical parameter	Symbol	Value
radius	r	2 m
density	ρ	1000 kg/m^3
mass	$m = \frac{2}{3}\pi r^3 \rho$	16755 kg
spring	$c = \pi r^2 \rho g$	123276 kg/m^3

Table 1: Physical characteristics of the buoy used as an example.

was initially referred to as efficiency, until it was found that a capture width of greater than one is possible [14]. When this occurs, it indicates that power is being captured from outside the section of wave-front that has the same width as the WEC. While this paper discusses capture width, the results and implications apply equally well to the relative capture width.

This paper presents new theory linking the formulas of capture width when excitation is monochromatic (sinusoidal) and when excitation is polychromatic. The monochromatic and polychromatic versions of capture width are linked by a spectral shape parameter, which the authors have named the spectral power fraction. The interaction of the spectral power fraction and the monochromatic capture width provides a useful insight into how WECs operate. An exploration of how the monochromatic capture width is influenced by the device's geometry (via the intrinsic impedance) and the control algorithm (via the PTO impedance) leads to theoretical confirmation of existing design and control strategies.

Section 2 defines the frequency domain (and thus linear post-transient) response of a generalised WEC. A specific geometry is described, and this supplies the values of the parameters in the generalised equation of motion. The generalised PTO force is defined. Specific control strategies are defined, and these supply the values of the PTO parameters in the generalised equation for PTO force.

The equations in §2 all involve continuous functions of frequency. This is because they describe the frequency domain representation of a process which is defined on a continuous and infinite time domain. When calculating hydrodynamic coefficients using experimental results, or using a numerical method such as the commercial code WAMIT [19], time and frequency must be discretised; hence the discrete Fourier transform (DFT) is used. The equations from §3 onwards are thus for discrete frequencies. Section 3 gives the DFT decompositions of wave energy transport and absorbed power. In the literature [7, 18] these decompositions are given for the continuous Fourier transform. Section 4 analyses the properties of capture width. Section 5 discusses how these newly introduced ideas apply to control strategies and the estimation of power production.

2. Frequency domain modelling

This section presents a generalised version of the well-known frequency domain model of a WEC. Non-linear systems can not be modelled in the frequency domain, so this approach only models the sub-set of linear behaviour. Non-linear terms are either linearised, or if the linear component is sufficiently small, not

included. It is important to distinguish the physical system (on the left in Fig. 2), which may often be non-linear, from the abstract model, which is linear (on the right in Fig. 2).

Equations are presented such that the forces, motions and transformation coefficients can be interpreted as either scalars (for a single degree of freedom) or vectors and matrices (for multiple degrees of freedom). The example used in this paper has only one degree of freedom, namely heave. Simplifications to the equation that are valid for heave only will be stated.

2.1. Geometry considered

A heaving spherical buoy, with the power take off (PTO) system reacting against the sea bed, will be considered. The non-dimensionalised radiation coefficients were first presented by Havelock [8]. Several authors [12, 5] have since used these results to demonstrate theoretical principles. This paper follows this precedent.

The model considered in this paper uses the parameters in Table 1, which give the radiation coefficients shown in Fig. 1. Net impedance as shown in Fig. 2 is used.

2.2. Generalised equation of motion

The generalised equation of motion of a linearised WEC is:

$$F_e(\omega) = i\omega[m + M(\omega)]U(\omega) + B(\omega)U(\omega) + \frac{c}{i\omega}X(\omega) + F_{pto}(\omega) \qquad (1)$$

where

$F_e(\omega)$	is the Fourier transform of the wave excitation force $f_e(t)$
i	is $\sqrt{-1}$
ω	is the circular frequency
$U(\omega)$	is the Fourier transform of velocity $u(t)$
m	is the dry mass of the WEC
$M(\omega)$	is the hydrodynamic added mass
$B(\omega)$	is the hydrodynamic added damping
c	is the linearised spring coefficient
$F_{pto}(\omega)$	is the Fourier transform of PTO force, $f_{pto}(t)$

Damping forces due to drag and losses in the PTO chain have not been included in this model. They are generally non-linear, so it is not possible to represent them with a frequency domain model. For small amplitude motions, the linear components of these forces are negligible, and are therefore not included in the model.

2.3. Intrinsic impedance

The excitation force and the PTO force can be considered external forces. All other terms can be considered *internal*, and thus intrinsic properties of a given geometry of WEC. These terms can be grouped:

$$F_e(\omega) = Z(\omega)U(\omega) + F_{pto}(\omega) \tag{2}$$

and described by the intrinsic impedance, $Z(\omega)$:

$$Z(\omega) = B(\omega) + i\left(\omega\left[m + M(\omega)\right] - \frac{c}{\omega}\right) \tag{3}$$

The intrinsic impedance is the transfer function between the excitation force and the unopposed WEC velocity, that is, the velocity when $Z_{pto} = 0$.

In this generalised model (3), the coefficient describing stiffness, c, represents any intrinsic spring in the system. In the specific example examined in this paper, it represents buoyancy spring. For a heaving cylinder, this is a function of the water density, ρ, acceleration due to gravity, g, and area of the WEC at the water surface, A_w : $c = \rho g A_w$. The buoyancy spring of a heaving spherical buoy is linearised by modelling A_w as constant with respect to heave displacement, as is the case for a heaving cylinder. As with all linearisations, this assumption is only applicable to small displacements.

The radiation problem

An oscillating body and the surrounding water apply a *radiation force* to each other as waves are created. It is useful to decompose radiation force (Fig. 2 - left: heaving buoy) into components in phase with velocity $U(\omega)$, and in phase with acceleration $A(\omega)$, (Fig. 2 - right: model):

$$F_r(\omega) = M(\omega)\ A(\omega) + B(\omega)\ U(\omega) \tag{4}$$

Writing (4) in phasor notation, the added mass and damping can be expressed as the radiation impedance:

$$Z_r(\omega) = i\omega M(\omega) + B(\omega) \tag{5}$$

This describes how a body's motion is impeded by the water due to the creation of waves.

Fig. 1 shows the radiation damping and added mass for the geometry defined in Table 1, as defined by [8].

2.4. The diffraction problem

The excitation coefficient, $W(\omega)$ defines the transfer function between the wave elevation and the exciting force:

$$F_e(\omega) = W(\omega)H(\omega) \tag{6}$$

where $H(\omega)$ is the Fourier transform of wave elevation $\eta(t)$.

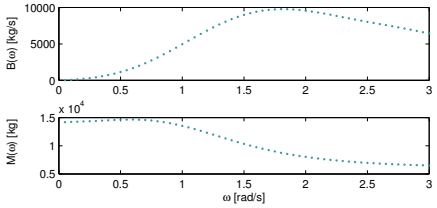

Figure 1: Radiation damping $B(\omega)$ and added mass $M(\omega)$ for a heaving hemisphere with a radius of 2m, as described in Table 1.

The diffraction coefficient is related to radiation damping via the Haskind relations [9]. For a heaving body with a vertical axis of symmetry:

$$\left|W(\omega)\right|^2 = \frac{4\rho g c_g(\omega, h)}{k(\omega, h)} B(\omega) \tag{7}$$

where $c_g(\omega, h)$ is the group velocity, $k(\omega, h)$ is the wave number, and h is the depth of the fluid.

2.5. Power take off impedance

For inclusion in the linear model (1), the PTO force must clearly also be linear. In general, the PTO force could contain forces proportional to displacement or its derivatives:

$$F_{pto}(\omega) = M_{pto}(\omega)\ A(\omega) + B_{pto}(\omega)\ U(\omega) + C_{pto}(\omega)\ X(\omega) \tag{8}$$

where $A(\omega)$, $U(\omega)$, $X(\omega)$ are the Fourier transforms of acceleration, velocity and displacement, and $M_{pto}(\omega)$, $B_{pto}(\omega)$, $C_{pto}(\omega)$ are the generalised inertial, damping, and spring PTO coefficients.

$M_{pto}(\omega)$ and $C_{pto}(\omega)$ do not represent physical lumps of mass and mechanical springs that are physically present in a WEC or its PTO system. Instead they represent components of the PTO force, placed by the primary power capture mechanism on the WEC, which have mass or spring-like properties. PTO mass and spring are differenct from adjustable mass or spring that can be used to control a WEC. These include changing the dry mass m, by adjusting the ballast, or changing the stiffness of a spring, such as the air-spring [13] used in the Archimedes Waveswing [1]. As discussed in §5.2, these adustable mass and spring terms form part of the intrinsic impedance. Although they can be used to control the WEC, they do not control the PTO force, so they do not form part of the PTO impedance.

Fig. 2 shows how the PTO force (left: buoy) is decomposed into forces proportional to mass, damping and spring (right: model). Equation (8) can be expressed more compactly as:

$$F_{pto}(\omega) = Z_{pto}(\omega)\ U(\omega) \tag{9}$$

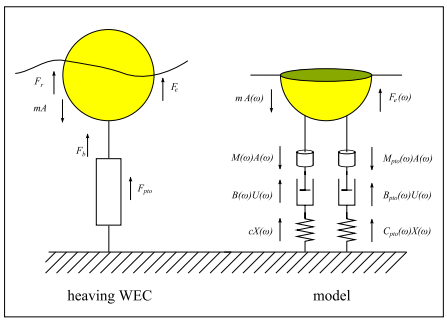

Figure 2: A heaving WEC experiencing radiation, inertial, buoyancy, PTO and excitation forces (left), and mass spring damper model (right).

where

$$Z_{pto}(\omega) = B_{pto}(\omega) + i\left(\omega M_{pto}(\omega) - \frac{C_{pto}(\omega)}{\omega}\right) \tag{10}$$

In the time domain, the PTO force (8) involves convolutions:

$$\begin{aligned} f_{pto}(t) &= z_{pto}(t) * u(t) \\ &= m_{pto}(t) * a(t) + b_{pto}(t) * u(t) + c_{pto}(t) * x(t) \end{aligned} \tag{11}$$

If causal versions of these convolutions are considered then it is possible to implement the PTO force using a filter. The resulting PTO force will then involve only past values of motion.

When the PTO settings, m_{pto}, b_{pto} and c_{pto}, are constants, rather than functions of frequency:

$$F_{pto}(\omega) = m_{pto}A(\omega) + b_{pto}U(\omega) + c_{pto}X(\omega) \tag{12}$$

the PTO force can be expressed as a weighted sum of the instantaneous acceleration, velocity and displacement:

$$f_{pto}(t) = m_{pto}a(t) + b_{pto}u(t) + c_{pto}x(t) \tag{13}$$

This could be implemented by multiplying sensor readings of acceleration, velocity and displacement by the relevant coefficients. The sum of the resulting signals could be used to drive the PTO. Equation (12) may also be expressed as (9). In this case:

$$Z_{pto}(\omega) = b_{pto} + i\left(\omega m_{pto} - \frac{c_{pto}}{\omega}\right) \tag{14}$$

Note that although the PTO settings do not vary with frequency, the PTO impedance does.

In equations (8) and (12) the PTO settings may have any value.

Net impedance

The equation of motion is complete when the linear PTO force is included. The net impedance is the combined intrinsic and PTO impedance:

$$\begin{aligned} F_e(\omega) &= [Z(\omega) + Z_{pto}(\omega)]\, U(\omega) \\ &= Z_{net}(\omega)\; U(\omega) \end{aligned} \tag{15}$$

Net impedance for acausal optimal control

For optimal power absorption, the PTO impedance must equal the complex conjugate of the intrinsic impedance at each frequency [7]:

$$\tilde{Z}_{pto}(\omega) = Z(\omega)^* \tag{16}$$

Here the tilde notation indicates that specific values have been defined to the PTO impedance, according to a given control algorithm. The following PTO settings are required to satisfy (8):

$$\begin{aligned} &\tilde{M}_{pto}(\omega) = -\left[m + M(\omega)\right] \\ &\tilde{B}_{pto}(\omega) = B(\omega) \\ &\tilde{C}_{pto}(\omega) = -c \end{aligned}$$

One of the consequences of optimal control (ensuring the ideal conditions to each frequency) is that the (inertial and damping) PTO settings are frequency dependent (filters). This frequency dependency is not what causes the optimal PTO force to be acausal. Frequency dependent PTO coefficients merely mean that the PTO force in the time domain is given by motions convolved with impulse response functions. If the overall impulse response function of the PTO force is causal, then the convolution will only involve past values of motion.

Equation (16) however, as well as defining the PTO coefficients, also defines the impulse response function of the PTO force as acausal [11]. This is because the inverse Fourier transform of the intrinsic impedance $z(t) = \mathcal{F}^{-1}\{Z(\omega)\}$ is a causal function of time, $z(t < 0) = 0$: the WEC only responds to instantaneous and previous values of motion. For any real function of time, $y(t) = \Re\{y(t)\}$, the Fourier transform has the following property:

$$Y^*(\omega) = Y(-\omega) \tag{17}$$

Equation (16) may be expressed as $\tilde{Z}_{pto}(\omega) = Z(-\omega)$, and the inverse Fourier transform of this $z(-t) = \mathcal{F}^{-1}\{Z(-\omega)\}$ is the time reversal of a causal function, which makes it acausal, $z(t > 0) = 0$.

For acausal optimal control the net impedance is:

$$\tilde{Z}_{net}(\omega) = 2B(\omega) \tag{18}$$

Net impedance for causal sub-optimal control

The optimal control described in (16) can be made causal by replacing $\tilde{z}_{pto}(t)$, which is an acausal function of time, with a delta function at the origin,

$\tilde{z}_{pto}\delta(t)$. The delta function is scaled by a constant, $\tilde{z}_{pto}$. Convolution with this scaled delta function is the same as multiplication by the scaling factor:

$$\tilde{z}_{pto}\delta(t) * u(t) = \tilde{z}_{pto}u(t) \tag{19}$$

Using this approximation, no future knowledge is required. The PTO is no longer optimal over all frequencies, so it is referred to as sub-optimal.

The Fourier transform of $\tilde{z}_{pto}\delta(t)$ gives PTO coefficients that are constants, as in (14), rather than functions of frequency (filters), as in (10). However, they are values of these constants can be chosen to give optimum power absorption at a single chosen frequency. This chosen frequency is termed the *peak frequency*, as it is usually the frequency at which the excitation or response has the most power. The PTO impedance at the peak frequency is chosen to be the complex conjugate of the intrinsic impedance at the peak frequency:

$$\tilde{Z}_{pto}(\omega_p) = Z^*(\omega_p) = B(\omega_p) - i\left(\omega_p\left[m + M(\omega_p)\right] - \frac{c}{\omega_p}\right) \tag{20}$$

Note that this defines the ideal PTO impedance at one frequency only. If both reactive PTO coefficients, m_{pto} and c_{pto}, are used, then the PTO coefficients are:

$$\begin{aligned}
&\tilde{m}_{pto} = -\left[m + M(\omega_p)\right] \\
&\tilde{b}_{pto} = B(\omega_p) \\
&\tilde{c}_{pto} = -c
\end{aligned}$$

Substituting these coefficients into (14) gives a PTO impedance (defined over all frequencies) of:

$$\tilde{Z}_{pto}(\omega) = B(\omega_p) - i\left(\omega\left[m + M(\omega_p)\right] - \frac{c}{\omega}\right) \tag{21}$$

and a net impedance of:

$$\tilde{Z}_{net}(\omega) = B(\omega) + B(\omega_p) - i\omega\left[M(\omega) - M(\omega_p)\right] \tag{22}$$

It is important to highlight that (14) and (10) represent generalised linear PTO impedance. Both can be used to generate causal PTO forces, although (10) can also be used to represent a non-causal PTO force. Equations (16) and (21) however represent linear PTO impedance for specific control actions. (16) is used with knowledge of the future state for acausal control, while (21) is used with knowledge of the instantaneous state for causal control. Not all authors differentiate between generalised PTO impedance and a specific PTO impedance in this manner; the distinction must then be deduced from the context.

3. Average power

Most experimental work involves the DFT. Discrete frequency notation (ω_j) is used for the remainder of this paper as this is usually necessary when analysing experimental results.

Plancherel's theorem, a generalised version of the better known Parseval's theorem, can be used to describe the product of two time domain functions, integrated over time, as the product of their Fourier transforms, integrated over frequency. For discrete quantities, the product of two time domain functions, summed over time, is related to the product of their DFTs, summed over frequency. As the DFT is defined for functions of time periodic with N, the DFT version of Plancherel's theorem is only valid for periodic functions. The formulations of the DFT and Plancherel's theorem used in this paper are (47) and (48) in Appendix A.

Plancherel's theorem can be used to write the power absorbed by a WEC, and the power incident on a WEC, as functions of frequency, rather than time.

3.1. Plancherel's theorem applied to absorbed power

The average power absorbed by a WEC over an interval of time containing N samples is the mean of the instantaneous power at each sample:

$$P_A = \frac{1}{N} \sum_{n=0}^{N-1} f_{pto}(t_n)\ u(t_n) \tag{23}$$

For periodic force and velocity, Plancherel's theorem (48) can be used to express the absorbed power as:

$$P_A = \sum_{j=0}^{N/2-1} P_A(\omega_j) = \frac{2}{N^2} \sum_{j=0}^{N/2-1} \Re\left\{F_{pto}(\omega_j)\ U^*(\omega_j)\right\} \tag{24}$$

The full derivation in Appendix A shows the origin of the $2/N^2$ coefficient. Multiplying a complex number by its complex conjugate gives the magnitude squared. So when the PTO force is a linear function of velocity (9), (24) can be reduced to:

$$P_A = \frac{2}{N^2} \sum_{j=0}^{N/2-1} B_{pto}(\omega_j)\ \left|U(\omega_j)\right|^2 \tag{25}$$

It is useful to express absorbed power as a function of hydrodynamic coefficients and wave elevation [16]. Combining (15) and (6), the velocity can be defined as:

$$U(\omega_j) = Z_{net}^{-1}(\omega_j)\ W(\omega_j)\ H(\omega_j) \tag{26}$$

We use Z_{net}^{-1} to indicate either scalar reciprocal or matrix inverse. Notation consistent with matrix algebra is used for easy comparison with equations for multiple degrees of freedom [16]. Substituting velocity (26) into the average absorbed power (25) gives:

$$P_A = \frac{2}{N^2} \sum_{j=0}^{N/2-1} B_{pto}(\omega_j)\ \left|Z_{net}^{-1}(\omega_j)\right|^2\ \left|W(\omega_j)\right|^2\ \left|H(\omega_j)\right|^2 \tag{27}$$

If the WEC is vertically symmetrical and moving in heave, then the diffraction coefficient can be eliminated. Substituting (7) into (27), absorbed power expands to:

$$P_A = \frac{8\rho g}{N^2} \sum_{j=0}^{N/2-1} \frac{B_{pto}(\omega_j)\ c_g(\omega_j, h)\ B(\omega_j)\ \left|H(\omega_j)\right|^2}{k(\omega_j, h)\ \left|Z_{net}(\omega_j)\right|^2} \tag{28}$$

Here net impedance is no longer a matrix, as the above equation is for a single degree of freedom.

The validity of these equations are as follows:

1. Equation (23) holds for the general case
2. Equation (24) holds for velocity and force that are periodic with the interval over which power is averaged
3. Equation (25) holds for PTO force that is linear with respect to velocity
4. Equations (27) and (38) hold for velocity that is linear with respect to wave elevation, as in (26)
5. Equation (28) holds for vertical symmetry and one degree of freedom; heave

The hydrodynamic parameters, and hence velocity, are never truly linear functions of wave elevation. However, all experimental and numerical models assume that the relationship is linear, and indeed experimental work is often intentionally limited to small motions so that behaviour falls within a linear regime, as defined by the experimenter.

Note that no restrictions on causality have yet been put into place. The most general definition of PTO impedance is used (10), which is why the PTO damping is expressed as $B_{pto}(\omega_j)$ rather than b_{pto}. No assumptions have been made about control principles which have assigned values to the PTO settings.

3.2. Plancherel's theorem applied to wave energy transport

From linear wave theory we know the power per metre wave front (also known as wave energy transport or power flux) of a regular wave with frequency ω_0 is [7]:

$$P_{IW}(\omega_0) = \frac{\rho g}{2} c_g(\omega_0, h)\ \left|H(\omega_0)\right|^2 \tag{29}$$

where $H(\omega_0)$ is the complex wave elevation, and the group velocity is defined by:

$$c_g(\omega_0, h) = \frac{g}{2\omega_0} D(\omega_0, h) \tag{30}$$

with $D(\omega_0, h)$ denoting the depth function:

$$D(\omega_0, h) = \tanh(k(\omega_0, h)h) \left[1 + \frac{2k(\omega_0, h)h}{\sinh(2k(\omega_0, h)h)}\right] \tag{31}$$

In deep water ($kh >> 1$) the depth function approaches unity and the group velocity is independent of depth:

$$c_g(\omega_0) \approx \frac{g}{2\omega_0} \tag{32}$$

Following the standard derivation of wave energy transport (pp 71-78 in [7]), and using the same adaptation to the DFT used in this paper for the absorbed power (Appendix A), Plancherel's theorem may be used to derive the DFT version of (29):

$$P_{IW} = \sum_{j=0}^{N/2-1} P_{IW}(\omega_j) = \frac{2\rho g}{N^2} \sum_{j=0}^{N/2-1} c_g(\omega_j, h) \left|H(\omega_j)\right|^2 \tag{33}$$

This is valid for periodic waves of small amplitude.

4. The properties of capture width

4.1. Definition of capture width

Capture width is a widely used measure of the performance of a WEC. This section presents new theory that can be used to explain the properties of capture width. All the theory is also relevant to the relative capture width, sometimes referred to as efficiency, which is the capture width normalised with respect to geometry.

Capture width is defined as the ratio of the power absorbed (P_A) to the wave energy transport (P_{IW}):

$$C_W = \frac{P_A}{P_{IW}} \tag{34}$$

For small periodic waves, wave energy transport may be written as a linear function of wave elevation (33). Assuming that velocity is periodic and linear with respect to wave elevation (conditions (ii)- (iv) in §3.1), absorbed power may also be written as a linear function of wave elevation (27). When all these conditions are satisfied, capture width (34) may be written as:

$$C_W = \frac{\sum_{j=0}^{N/2-1} B_{pto}(\omega_j) \left|Z_{net}^{-1}(\omega_j)\right|^2 \left|W(\omega_j)\right|^2 \left|H(\omega_j)\right|^2}{\sum_{l=0}^{N/2-1} \rho g c_g(\omega_l, h) \left|H(\omega_l)\right|^2} \tag{35}$$

In monochromatic experiments at the frequency ω_0, only one term in each sum is non-zero. The result is the monochromatic capture width:

$$C_W^0(\omega_0) = \frac{P_A(\omega_0)}{P_{IW}(\omega_0)} \tag{36}$$

Substitution of (33) and (27) into this gives:

$$C_W^0(\omega_0) = \frac{B_{pto}(\omega_0) \left|Z_{net}^{-1}(\omega_0)\right|^2 \left|W(\omega_0)\right|^2}{\rho g c_g(\omega_0, h)} \tag{37}$$

Following on from the assumption that both absorbed power and wave energy transport can be written as linear functions of wave elevation, absorbed power may then be expressed as a linear function of wave energy transport. Rearranging (27) as a function of (33) gives:

$$\begin{aligned} P_A &= \sum_{j=0}^{N/2-1} \frac{B_{pto}(\omega_j)\ \left|Z_{net}^{-1}(\omega_j)\right|^2\ \left|W(\omega_j)\right|^2}{\rho g c_g(\omega_j, h)} P_{IW}(\omega_j) \\ &= \sum_{j=0}^{N/2-1} G(\omega_j)\ P_{IW}(\omega_j) \end{aligned} \tag{38}$$

where $G(\omega_j)$ is a linear operator. From (37) it can be seen that $G(\omega_j)$ is a function of frequency whose value is defined as the monochromatic capture width at that frequency, $C_W^0(\omega_j)$. Absorbed power may thus be written as:

$$P_A = \sum_{j=0}^{N/2-1} C_W^0(\omega_j)\ P_{IW}(\omega_j) \tag{39}$$

Substituting this into (34) gives:

$$C_W = \sum_{j=0}^{N/2-1} C_W^0(\omega_j) \frac{P_{IW}(\omega_j)}{P_{IW}} \tag{40}$$

Introducing a new term, the *spectral power fraction*:

$$P_f(\omega_j) = \frac{P_{IW}(\omega_j)}{P_{IW}} \tag{41}$$

allows the polychromatic capture width to be expressed as:

$$C_W = \sum_{j=0}^{N/2-1} C_W^0(\omega_j)\ P_f(\omega_j) \tag{42}$$

From this equation, it can be seen that capture width is a measure of the interaction between the monochromatic capture width (35), $C_W^0(\omega_j)$, which is a property of the device, and the spectral power fraction (41), $P_f(\omega_j)$, which is a property of the shape of the incident wave spectrum. These properties are now examined in turn.

4.2. Spectral property: power fraction

The spectral power fraction (41) is a function that gives the fraction of the total wave energy transport contained in each frequency component for a given wave spectrum. Its derivation assumed that the spectrum was defined for periodic seas, so it cannot be directly related to spectral measurements of real seas.

Substitution for wave energy transport (33) and group velocity (30) gives:

$$P_f(\omega_j) = \frac{\frac{D(\omega_j,h)}{\omega_j}\left|H(\omega_j)\right|^2}{\sum_{l=0}^{N/2-1} \frac{D(\omega_l,h)}{\omega_l}\left|H(\omega_l)\right|^2} \tag{43}$$

This equation highlights three important points. The first is that power fraction remains unchanged if the wave elevation spectrum is scaled, using the same scaling factor on each amplitude component. This means that power fraction characterises the spectral shape of the incident wave power spectrum. The second point is that power fraction is a function of water depth. The third is that power fraction depends on the number of points in the DFT. This is because the magnitude of the elevation component $\left|H(\omega_j)\right|$ (the numerator), depends upon the width of the bin, whereas the wave energy transport (the denominator) is the same, regardless of bin width. Nevertheless, the sum of the components of $P_f(\omega_j)$ over a given band of frequencies will always be the same, regardless of the bin width.

4.3. Device property: monochromatic capture width

In (42) it was shown that capture width measured the interaction of a spectral property and a device property. This device property is a function giving the monochromatic capture width at each frequency:

$$C_W^0(\omega_j) = \frac{P_A(\omega_j)}{P_{IW}(\omega_j)} \tag{44}$$

This definition follows from (39). The monochromatic capture width function may be expanded as in (37) with (ω_j) for (ω_0).

Note that in (37) the monochromatic capture width does not contain wave amplitude terms. It does not depend on the wave spectrum; only on device characteristics. The polychromatic capture width (42) however depends on both device characteristics and the shape of the wave spectrum. This important distinction between the monochromatic and polychromatic capture widths should not be forgotten. The distinction has been noted by some researchers, for example Delauré and Lewis [3], who described them as the steady state and spectral efficiencies. To our knowledge we are the first to show (40) how these capture widths are related to one another.

If the water is deep (32), and if the WEC is vertically symmetrical and moving in one degree of freedom: heave (7); then the monochromatic capture width reduces to:

$$C_W^0(\omega_0) = \frac{4gB_{pto}(\omega_0)\ B(\omega_0)}{\omega_0^2\ \left|Z_{net}(\omega_0)\right|^2} \tag{45}$$

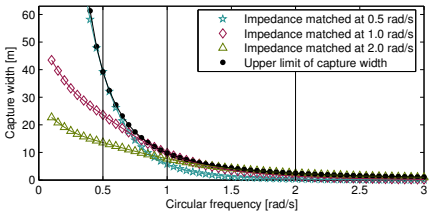

Figure 3: Capture width for three different tuned frequencies compared to the upper limit. Inertial, damping and spring PTO coefficients were used, and amplitude limits were not imposed.

4.4. The effect of PTO on the capture width

In (37) we see that the monochromatic (and hence polychromatic) capture width depends on both the geometry (W and Z) and the choice of PTO (Z_{pto}) (see (15)). As any plot of capture width is specific to a particular choice of PTO impedance, care must be taken when producing or interpreting plots of capture width. While capture width is defined for an arbitrary PTO impedance, in order to plot it, a specific value of PTO impedance must be chosen.

Some authors indicate that capture width depends on the PTO impedance by plotting several curves to show the effect of different PTO options. Fig. 3 is an example of several plots of capture width, each with a different value of PTO impedance. The spherical buoy described in Table 1 is considered, and capture width is calculated using (45). The large open markers show the capture width for PTO impedance given by causal sub-optimal control (21). The impedance is matched at a single frequency, with each large open marker indicating impedance matching at a different value of operating frequency, ω_p.

The line with small solid markers in Fig. 3 shows another commonly used convention for plotting capture width. The solid markers are the capture width for a monochromatic system, $C_W^0(\omega_0)$, when the PTO impedance has been chosen for optimal control. Optimal control is causal in the special case of monochromatic behaviour. Note that for polychromatic systems, the solid markers also indicate the component of the device property $C_W^0(\omega_j)$, when the PTO has been chosen for acausal optimal control. In monochromatic tests, the solid markers are realisable without knowledge about the future. In polychromatic tests, they indicate an upper limit that is only attainable with future knowledge [11]. Some authors [5] helpfully emphasise that this is an upper limit, using adjectives such as 'maximum'. This [5] is a maximum not only because amplitude limits (as imposed in [12]) have not been considered, but also because the chosen PTO impedance assumes acausal optimal control. Many authors do not however indicate that this an upper limit when using PTO impedance optimised at each frequency, so when viewing a capture width plot, it is important to discern what value of PTO impedance was used.

The upper limit of capture width should not be used to calculate polychromatic capture width (42). This is because optimising PTO at each frequency amounts to acausal optimal control, which can not be implemented in real time.

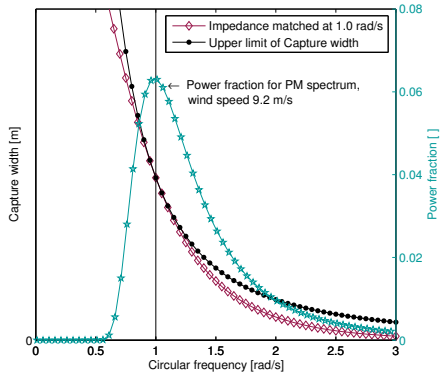

Figure 4: Monochromatic capture width for a WEC with impedance matched at 1 rad/s, and power fraction with a peak at 1 rad/s, for a PM spectrum associated with a wind-speed of 9.2m/s, and discrete bins separated by 0.01 rad/s.

Estimating annual power absorption (§5.3) using capture width calculated in this manner will give the power that would be absorbed if acausal control were somehow possible. Rather, capture width using the PTO impedance that is applied in polychromatic waves (such as those indicated by open markers in Fig. 3), should be used.

4.5. Interaction between spectral and device properties

While the monochromatic capture width has a different value at each frequency bin, the polychromatic capture width is not a function of time or frequency, but has a single value. This is found by adding components at each frequency: $C_W = \sum_{j=0}^{N/2-1} C_W(\omega_j)$. Each frequency component is the monochromatic capture width scaled by the power fraction (42). This multiplication can be visualised by plotting power fraction and monochromatic capture width on the same axes (Fig. 4). The monochromatic capture width acts like a window for the power fraction. The ideal case would be high values of monochromatic capture width coinciding with high values of power factor. Indeed, the polychromatic capture width is effectively a measure of how well matched the monochromatic capture width and the power fraction are.

Although the monochromatic and polychromatic capture widths share the same conceptual definition, they have different formulations, as seen in (42). They may be compared by considering the power fraction of a monochromatic wave: $P_f = \delta(\omega_j - \omega_0)$. This is a a delta function with a value of one at ω_0, and a value of zero at all others. Summation of the product of a delta function and the monochromatic capture width (function of frequency), gives the value of monochromatic capture width at ω_0:

$$C_W = \sum_{j=0}^{N/2-1} C_W^0(\omega_j)\ \delta(\omega_j - \omega_0) = C_W^0(\omega_0) \tag{46}$$

For a monochromatic wave, the (total) capture width *is* the monochromatic capture width. If a suitable PTO impedance is chosen, then the capture width can be maximised for that frequency. However, if the same energy were spread out over many frequencies, and PTO impedance was chosen to maximise the capture width at the frequency with the most energy, then on either side of the tuned frequency, the capture width would drop away from the maximum. Thus for tuned PTO impedance, capture width will always be higher for a monochromatic wave than for a spectrum of equivalent energy. For example, monochromatic capture width plotted against period ($2\pi/\omega_0$) would be higher than polychromatic capture width plotted against energy period for a spectrum with the same energy content [15] as the monochromatic wave.

It is worth keeping in mind that polychromatic capture width plotted against energy period is only valid for a particular shape of spectrum (power fraction). In general, a peakier spectrum will result in a higher polychromatic capture width than a broader spectrum, as more energy will lie at frequencies where there is better absorption.

It has been known for some time that it is preferable for the monochromatic capture width (given by the chosen PTO impedance) to coincide with the incident wave spectrum. Indeed, plotting capture width and a spectral parameter on the same graph is not new [7, 18]. What is new however, is a precise mathematical relationship between the parameters being plotted. The product of the spectral parameter and the monochromatic capture width shown in Fig. 4 yields the performance in mixed seas.

5. Discussion

5.1. Matching spectral and device properties with PTO

Fig. 4 shows that it is preferable for the monochromatic capture width to be optimised at the frequency for which the spectral power fraction is the highest. Fig. 3 shows that the PTO impedance can be used to optimise the monochromatic capture width at one frequency. Thus, by matching the impedance at the frequency where the waves have the most power, the spectral and device properties introduced in §4.2 and §4.3 can be matched so as to optimise the capture width.

In Fig. 3, it can be clearly seen that the monochromatic capture width equals the upper limit defined by acausal optimal control (solid markers) only at the operating frequency ω_p (indicated by the vertical bars). Note that for this geometry (Table. 1) the choice of tuning frequency for impedance matching using (21) does not make a significant difference to the monochromatic capture width. This was noted by [10] who compared 'variable and constant coefficient systems', corresponding to the acausal optimal control and causal sub-optimal control described in this paper.

The monochromatic capture width for impedance matching (causal control) equals the upper limit at ω_p. At all other frequencies, it is less than the upper limit. The drop from the upper limit will depend upon how easily the intrinsic

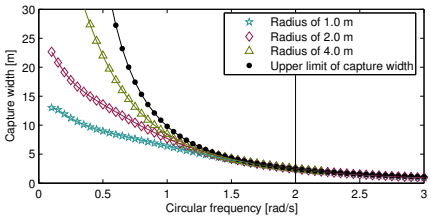

Figure 5: Capture width for a control strategy that matches impedance at one frequency (open markers), 2 rad/s in this case, compared to the upper limit (solid markers). The upper limit is independent of the size of the WEC. The capture width for impedance matching at one frequency is shown for three different sizes of WEC.

impedance can be matched using the available PTO coefficients. The upper limit shown in Fig. 3 is that defined by Evans [4]. In the case of heave, this upper limit is $\lambda/2\pi$, where λ is the wavelength of a wave at a given frequency. The upper limit of the monochromatic capture width (using acausal control) is determined by directionality and modes of motion, and does not depend on the scale of the geometry. However, the monochromatic capture width which is achievable using causal control depends on the intrinsic impedance. It is affected by the scale of the geometry. Fig. 5 shows monochromatic capture width (45) for three different sizes of the same heaving buoy, with impedance matched at the same frequency (21). For the larger buoy, the monochromatic capture width is close to the upper limit for a broader band of frequencies than is the case for the smaller buoys.

5.2. Matching spectral and device properties with geometry

Much research on the control of WECs is focussed on choosing the best values of PTO impedance for a given, fixed, intrinsic impedance. However, there is a limit to how much the PTO can change the capture width for the following reasons:

1. There are costs associated with reactive power: capital costs and energy losses.

2. The upper limit of the monochromatic capture width is determined by directionality and modes of motion.

3. This upper limit is not achievable in polychromatic seas: it requires exact knowledge of the near future state. The monochromatic capture width achievable without future knowledge is always less than the upper limit. At best it can equal the upper limit at one frequency only.

4. At any other frequency, the difference between the monochromatic capture widths achieved with causal control, and aspired to with acausal control,depends on the intrinsic impedance.

Optimising PTO impedance is only tackling one small part of the problem; a more holistic approach is to also consider the geometry of the WEC. In this context, a change in geometry refers to anything that alters the intrinsic impedance Z or diffraction coefficient W. Geometry control used along with impedance matching (causal sub-optimal control) has the potential to be more effective than impedance matching alone. The importance of this has been known for some time, but it is useful to have a performance indicator like capture width to explain why this should be the case.

The geometry can be considered at the design stage and during operation. At the design stage, it is important to choose a geometry for which implementable control, such as impedance matching at one frequency, results in a good (monochromatic) capture width relative to the expected sea-states. Design approaches that match the natural resonance with the sea state, or ensure broad response, fall into this category.

During operation, it is possible to alter physical properties to improve the match of the capture width with the sea-state. There are two mechanisms for this. Either the directionality or modes of motion can be used to change the upper limit of monochromatic capture width, or the intrinsic impedance can be changed so that it is easier to match using a given control strategy. In situ geometry control could include:

- aligning a directional device with respect to the principle wave direction
- altering mechanical mass or spring coefficients (often referred to as 'slow tuning')
- changing the configuration of structural members relative to each other or the water surface
- changing the degrees of freedom of motion with respect to the water surface

These approaches are well known and are receiving attention from device developers. The Archimedes Waveswing incorporates air springs [13]. The Pelamis controls its angle of motion with respect to the water surface by changing the ratio of PTO forces in two orthogonal degrees of freedom [20]. Pelamis also passively aligns itself to the waves, but this is to limit rather than maximise power, by ensuring it remains in attenuator configuration rather than terminator configuration.

5.3. Annual power estimation

Generalised spectra

A set of generalised spectra describe the typical annual distribution of sea-states in a given location. Measured spectra gathered at regular intervals over the course of a year are grouped into subsets according to characteristics such as the number of spectral peaks, the positions and heights of these peaks and bandwidth. The spectra in each subset are averaged to produce a generalised

spectrum which represents that subset. The size of the subset indicates the annual occurrence of a given generalised spectra. Time series of typical sea states can later be synthesised using randomly generated phase. An example of a group of generalised spectra is the South Uist 399 data set [2]. The measured data may come from one year, in which case that year is assumed to be typical.

The measured spectra are generated using measured wave records of surface elevation. Each sampled wave record (usually half an hour to two hours in length) is first processed to remove errors. Noise reduction techniques are then implemented, such as multiplication with a tapered window function. The wave record is transformed using the DFT. The measured spectra consist of the magnitude of the DFT, or the spectral density. The phase is discarded.

Validity of annual power estimation

Equation (39), or variants thereof, are often used [3, 16] to estimate annual power capture for a set of generalised spectra. There are several reasons why this is only an approximation to the power that would be absorbed at the site described by the generalised spectra:

- this equation is only valid for conditions (ii)-(iv) outlined in §3.1, yet measured seas are never periodic with the measurement record, and sea-states are often big enough to induce non-linear WEC response
- sea-states vary year by year
- generalised spectra are not the measured spectra
- the measured spectra are not the frequency domain equivalents of the measured wave records; noise reduction techniques have removed the equivalence of the time and frequency domains
- forces due to tides and waves created by neighbouring bodies are not considered
- PTO impedance is often optimised at a frequency, ω_p, calculated taking the whole spectrum into account; an option not available in real-time operation

Furthermore, calculating absorbed power using PTO impedance that has been optimised at each frequency will give an over-estimation. The absorbed power calculated in this manner is in fact the upper limit of power that would have been absorbed if acausal optimal control (knowledge of future state) were possible.

6. Conclusions

Capture width is a powerful performance indicator for wave energy converters (WECs). The polychromatic capture width is a function of the interaction of the monochromatic capture width, a property of the device, and the power fraction, a property of the sea-state. A good capture width is an indication of

a good overlap of these two properties. This confirms the design principle of choosing a WEC with a natural period that coincides with the energy period of the design spectrum.

The relationship between the monochromatic and polychromatic capture widths was presented. Using a linear PTO to optimise performance for a particular frequency can only move the monochromatic capture width within the upper limits defined by the geometry. This suggests that research on control of WECs should not be limited to PTO control only, but should also include geometry control. This is specially important as several leading device developers [20, 13] include it in their control strategies. The distinction between PTO control and geometry control was drawn to emphasise that they are fundamentally different techniques that affect the capture width in different ways.

The definition of polychromatic capture width as a function of device and sea-state properties only applies under certain conditions. It is valid when Fourier decompositions of wave energy transport and absorbed power can be made; waves must be small and WEC response must be linear. When the hydrodynamic parameters are defined at discrete frequencies, and the sea-state and response are measured at discrete time intervals, then the relationship between the time and frequency domains is the DFT. The DFT form of capture width (35) is only valid when the time series used to find the wave spectrum and the response of the WEC are periodic with the DFT record. These restrictions limit the accuracy with which capture width, calculated from hydrodynamic coefficients of a given WEC, can be used to estimate the annual power production of a WEC. The method for annual power production using generalised spectra was described, and sources of error and uncertainty were discussed.

Acknowledgements

The authors thank Jørgen Hals and David Forehand for advice and proofreading. The first author was supported by the EPSRC funded SuperGen-Marine program. The second author was supported by the EPSRC funded SuperGen-Amperes program. This work was carried out in the Joint Research Institute with the Heriot-Watt University, a part of the Edinburgh Research Partnership, which is supported by the Scottish Funding Council.

A. Decomposition of absorbed power

A.1. Plancherel's theorem depends on the form of the DFT

For the most common form of the DFT [17] and its inverse transform:

$$X(\omega_j) = \frac{1}{N} \sum_{n=0}^{N-1} x(t_n) e^{-i2\pi jn/N}$$
$$x(t_n) = \sum_{j=0}^{N-1} X(\omega_j) e^{j2\pi jn/N} \tag{47}$$

Plancherel's equation is:

$$\sum_{n=0}^{N-1} a(t_n)\ b^*(t_n) = \frac{1}{N} \sum_{j=0}^{N-1} A(\omega_j)\ B^*(\omega_j) \tag{48}$$

There are other conventions for describing the DFT and its inverse. In the symmetrical (unitary) form, the DFT and its inverse transform are:

$$\begin{aligned} X(\omega_j) &= \frac{1}{\sqrt{N}} \sum_{n=0}^{N-1} x(t_n) e^{-i2\pi jn/N} \\ x(t_n) &= \frac{1}{\sqrt{N}} \sum_{j=0}^{N-1} X(\omega_j) e^{j2\pi jn/N} \end{aligned} \tag{49}$$

in which case, Plancherel's equation is defined as:

$$\sum_{n=0}^{N-1} a(t_n)\ b^*(t_n) = \sum_{j=0}^{N-1} A(\omega_j)\ B^*(\omega_j) \tag{50}$$

Plancherel's theorem is used to express the power absorbed by a linear WEC as a function of the DFT of the (PTO mechanism's) velocity. The coefficient of the power decomposition depends on which form of DFT is assumed. However, the same is true when the wave energy transport is expressed as a function of wave elevation. As capture width is the ratio of absorbed power to incident power (wave energy transport), the coefficients that arise from different forms of the DFT, i.e. (47) or (49), cancel in (35). Likewise, any coefficients resulting from a different form of Fourier transform, such as the discrete time Fourier transform [16] or the continuous Fourier transform (for example [6]), cancel when calculating the ratio of absorbed to incident power.

A.2. DFT Decomposition of absorbed power

Average absorbed power is usually expressed as a function of the complex amplitude, or the continuous Fourier transform, of (the PTO system's) velocity [7, 18]. In an experimental system where velocity is measured or calculated at discrete points in both the time and frequency domains, the transformation between domains is the DFT. It is thus useful to express averaged absorbed power in terms of the DFT of velocity.

The average absorbed power over an interval of time containing N samples is the mean of the instantaneous power at each sample:

$$P_A = \frac{1}{N} \sum_{n=0}^{N-1} f_{pto}(t_n) u(t_n) \tag{51}$$

As both force and velocity are real, either may be written as it's complex conjugate. When force (9) and velocity are periodic over the interval N, the DFT

version of Plancherel's theorem [48] can be used to express the absorbed power as:

$$P_A = \frac{1}{N^2} \sum_{j=0}^{N-1} F_{pto}(\omega_j) U^*(\omega_j) \tag{52}$$

Assuming that N is an even number, which is always the case for the Fast Fourier transform implementation of the DFT, this sum can thus be split into two sums with limits up to and from $N/2$:

$$P_A = \frac{1}{N^2} \left(\sum_{j=0}^{N/2-1} F_{pto}(\omega_j) U^*(\omega_j) + \sum_{j=N/2}^{N-1} F_{pto}(\omega_j) U^*(\omega_j) \right) \tag{53}$$

This is useful because the DFT is periodic with frequency. The information in the bins $N/2$ to $N-1$ is exactly the same as that in the bins from $-(N/2-1)$ to 0. The limits on the second sum can be changed to reflect this:

$$P_A = \frac{1}{N^2} \left(\sum_{j=0}^{N/2-1} F_{pto}(\omega_j) U^*(\omega_j) + \sum_{j=-(N/2-1)}^{0} F_{pto}(\omega_j) U^*(\omega_j) \right) \tag{54}$$

Reversing the frequency limits on the second sum gives it the same limits as the first sum:

$$P_A = \frac{1}{N^2} \left(\sum_{j=0}^{N/2-1} F_{pto}(\omega_j) U^*(\omega_j) + \sum_{j=0}^{N/2-1} F_{pto}(-\omega_j) U^*(-\omega_j) \right) \tag{55}$$

When the time domain is real, as is the case here, taking the complex conjugate of the frequency domain is the same as reversing the frequency axis. The DFT form of this relation, (17), is $Y^*(\omega_j) = Y(-\omega_j)$. Applying this to the terms in the second sum gives:

$$P_A = \frac{1}{N^2} \left(\sum_{j=0}^{N/2-1} F_{pto}(\omega_j) U^*(\omega_j) + \sum_{j=0}^{N/2-1} F^*_{pto}(\omega_j) U(\omega_j) \right) \tag{56}$$

The second sum is now the complex conjugate of the first sum. Any function added to its complex conjugate gives twice the real part of that function:

$$P_A = \frac{2}{N^2} \sum_{j=0}^{N/2-1} \Re \left\{ F_{pto}(\omega_j) U^*(\omega_j) \right\} \tag{57}$$

References

[1] `http://www.awsocean.com/`.

[2] J. A. Crabbe. Synthesis of a directional wave climate. In B. Count, editor, *Power from Sea Waves*, pages 41–74. Academic Press, London, UK, 1980.

[3] Y. Delauré and A. Lewis. 3d hydrodynamic modelling of fixed oscillating water column wave power plant by a boundary element methods. *Ocean Engineering*, 30(3):309–330, 2003.

[4] D. V. Evans. A theory for wave-power absorption by oscillating bodies. *J. Fluid Mech.*, 77(1):1–25, 1976.

[5] D. V. Evans. Maximum wave-power absorption under motion constraints. *Applied Ocean Research*, 3(4):200–203, 1981.

[6] D. V. Evans, D. Jeffrey, S. H. Salter, and J. Taylor. Submerged cylinder wave energy device:theory and experiment. *Applied Ocean Research*, 1(1):3–12, 1979.

[7] J. Falnes. *Ocean Waves and Oscillating Systems.* Cambridge University Press, 2002.

[8] T. Havelock. Waves due to a floating sphere making periodic heaving oscillations. *Proc R. Soc.*, 231(1184):1–7, 1955.

[9] J. N. Newman. The interaction of stationary vessels with regular waves. In *Proc 11th Symp Naval Hydrod*, pages 491–501, London, 1976.

[10] S. Niato. Wave generation and absorption in wave basins: theory and application. *International Journal of Offshore and Polar Engineering*, 16(2):81–89, 2006.

[11] S. Niato and S. Nakamura. Wave energy absorption in irregular waves by feedforward control system. In D. Evans and A. F. de O. Falcão, editors, *Hydrodynamics of Ocean Wave-Energy Utilization*, pages 269–280. Springer Verlag, Lisbon, 1985.

[12] D. Pizer. Maximum wave-power absorption of point absorbers under motion constraints. *Applied Ocean Research*, 15(4):227–234, 1993.

[13] H. Polinder, M. E. C. Damen, and F. Gardner. Linear PM generator system for wave energy conversion in the AWS. *IEEE transaction on Energy Conversion*, 19(3):583–589, 2004.

[14] S. Salter. Looking back. In J. Cruz, editor, *Ocean Wave Energy*, pages 7–38. Springer, 2008.

[15] S. H. Salter and C. P. Lin. Wide tank efficiency measurements on a model of the sloped IPS buoy. In *Proc of the 3rd European Wave Energy Conference*, pages 200–206, Patras, 1998.

[16] D. J. Skyner. Solo duck linear analysis. Technical report, Edinburgh Wave Power Project, 1987.

[17] S. W. Smith. *The Scientist and Engineer's Guide to Digital Signal Processing.* California Technical Pub, 1998.

[18] G. Thomas. The theory behind the conversion of ocean wave energy: A review. In J. Cruz, editor, *Ocean Wave Energy*, pages 41–91. Springer, 2008.

[19] `http://www.wamit.com/`.

[20] R. Yemm. Full-scale wecs: Pelamis. In J. Cruz, editor, *Ocean Wave Energy*, pages 304–321. Springer, 2008.